Experimental and theoretical investigation of generation of a cross-polarized wave by cascading of two different second-order processes

G. I. Petrov

Faculty of Physics, University of Sofia, 5 J. Bourchier Boulevard, BG-1164, Sofia, Bulgaria

O. Albert

Laboratoire d'Optique Appliquée Unité Mixte de Recherche 7639, Centre National de la Recherche Scientifique–Ecole Nationale Supérieure de Techniques Avancées, Ecole Polytechnique, Centre de l'Yvette, 91761 Palaiseau Cedex, France

N. Minkovski

Faculty of Physics, University of Sofia, 5 J. Bourchier Boulevard, BG-1164, Sofia, Bulgaria

J. Etchepare

Laboratoire d'Optique Appliquée Unité Mixte de Recherche 7639, Centre National de la Recherche Scientifique–Ecole Nationale Supérieure de Techniques Avancées, Ecole Polytechnique, Centre de l'Yvette, 91761 Palaiseau Cedex, France

S. M. Saltiel

Faculty of Physics, University of Sofia, 5 J. Bourchier Boulevard, BG-1164, Sofia, Bulgaria

Received April 12, 2001; revised manuscript received September 13, 2001

A nonlinear optical effect in which a linearly polarized wave propagating in a single quadratic medium is converted into a wave that is cross polarized to the input wave is investigated theoretically and observed experimentally in β-barium borate crystal. It is proved that this effect is a result of cascading of two different second-order processes. It starts with the generation of an extraordinary second-harmonic wave by type I interaction and is followed by type II difference-frequency mixing between the second-harmonic wave and the ordinary fundamental wave. The experiment was performed (a) for phase-matched type I interaction and non-phase-matched type II interaction and (b) for non-phase-matched type I interaction and phase-matched type II interaction. The observed generation of a cross-polarized wave is to our knowledge the only cubic effect whose first manifestation has been observed in quadratic crystal.

OCIS codes: 190.4360, 190.4380, 200.4740, 230.5440.

1. INTRODUCTION

Second-order cascading (SOC) can be formally divided in two groups. The first is conventional SOC, in which the effect results from cascading of several subprocesses that belong to a single quadratic process.[1–3] For example, accumulation of a nonlinear phase shift encountered by a wave at a frequency ω associated with type I second-harmonic generation is the result of the cascading of $\omega + \omega = 2\omega$ and $2\omega - \omega = \omega$ subprocesses. This type of SOC is governed by a single phase-matching parameter $\Delta k = k_2 - 2k_1$ that occurs two times. Because of this SOC, many cubic effects such as nonlinear phase shift,[4] pulse compression,[5,6] and soliton propagation[7–9] can be observed in quadratic media at lower pump levels than in centrosymmetric media.

The second type of SOC, frequently called multistep second-order cascading, involves two different second-order processes (TDSOPs), each one of which is characterized by its own phase-matching parameter. Like conventional SOC, cascading of TDSOPs also simulates a third-order process. Investigations and experiments with the objective of obtaining phase-matched third-harmonic generation (THG) in a single crystal[10–20] exemplify this possibility. There, THG is the result of cascading of $\omega + \omega = 2\omega$ and $2\omega + \omega = 3\omega$ processes. Moreover, several recent investigations predicted that effects based on self- and cross-phase modulation, like the accumulation of nonlinear phase shifts[21,22] and soliton propagation,[23–27] also can be observed with cascading of TDSOPs. In processes that deal with cascading of TDSOPs, special attention has been paid to the case in which the interacting waves involved concern only two frequencies,[22,23,28–32] which is frequently called two-color multistep cascading.[22,23] Another frequency-shifting effect, which

0740-3224/2002/020268-12$15.00

uses more than two frequencies and has important applications in the optical communications industry, is a result of cascading from $\omega + \omega = 2\omega$ and $2\omega - \omega_a = \omega_b$. Obtaining such frequency shifting by use of a single quadratic crystal[33–35] is a significant demonstration of the capability of TDSOP cascading to simulate $\chi^{(3)}$ effects with much higher efficiency. In all cases, the cubic effects observed in quadratic media from both types of cascading reproduce cubic effects that have already been observed in centrosymmetric media.

The cascade processes described so far involve energy conversion, nonlinear phase shifts, or both. In this paper we investigate both theoretically and experimentally another TDSOP cascading effect that deals with polarization manipulation. It corresponds to the generation of a cross-polarized wave (XPW). According to our knowledge this multistep effect (for preliminary experimental results see Ref. 36) was never observed before. Moreover, we believe that it is by now the only cubic effect whose first manifestation has been observed in a quadratic crystal. In the process of XPW generation, three degenerate linearly polarized fields carried by the same beam generate, through an effective cubic nonlinearity, a new wave at the same frequency but polarized in the plane perpendicular to the input wave. The nonlinear interaction that we investigate is therefore a direct way to generate a XPW. The basic idea is totally different from that of all known linear and nonlinear[37–42] methods that deal with polarization rotation. As a matter of fact, the known methods of polarization rotation are based on a succession of several steps: splitting of an input beam into two beams in an anisotropic crystal, manipulation of the phase difference of the two beams through the birefringence effect (in linear optical methods) or accumulation of nonlinear phase shift (in nonlinear optical methods), and subsequent interferometric recombination of the split incoming beams.

In the past, the effect of XPW generation as a result of anisotropy of the $\chi^{(3)}$ tensor $\Delta\chi^{(3)} = \chi^{(3)}_{xxxx} - 3\chi^{(3)}_{xxyy}$ and nonvanishing $\chi^{(3)}_{xxxy}$ and $\chi^{(3)}_{xyyy}$ was considered in a series of publications by Zheludev and co-workers (see, e.g., Refs. 43–45). This effect, called by them self-induced ellipticity, together with the effect of nonlinear optical polarization rotation described by the anisotropy of the Im $\chi^{(3)}$ and of high-order gyrotropy tensor $\gamma^{(3)}_{ijklm}$, covers the interesting field known as nonlinear optical activity.[43] However, according to our knowledge, the effect of $\chi^{(3)}$ self-induced ellipticity has not been observed in volume experiments.

This paper is organized as follows: In Section 2 a simplified analysis of the conditions for nonlinear generation of a XPW is presented. Section 3 contains a more-detailed theoretical analysis, with special attention paid to the cases when at least one of the processes is phase matched. Section 4 is devoted to the experimental observation of the generation of a XPW in a β-barium borate (BBO) crystal and to a discussion of the results.

2. BASIC IDEA

The main idea for the generation of a XPW is sketched in Fig. 1. The polarization plane of the input wave is tuned in a way such that in the linear regime only one of the two

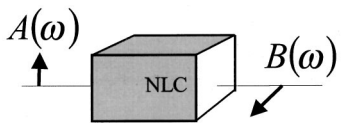

$$B(\omega) = \frac{\chi^{(2)}_{eff,1}\chi^{(2)}_{eff,2}}{\Delta k} A(\omega)A(\omega)A(\omega)$$

Fig. 1. Sketch for generation of a XPW based on cascading of two different second-order processes: NLC, nonlinear crystal.

allowed eigenwaves, e.g., an ordinary (o) or an extraordinary (e) component, propagates in the quadratic medium. The overall process used for generating a wave whose polarization vector is perpendicular to the polarization vector of the input wave consists of two steps: second-harmonic generation (SHG) from two identical fundamental waves and difference-frequency mixing (DFM) in which the second harmonic (SH) is downconverted back to the XPW at the fundamental frequency. To illustrate the principle of generation of a XPW, let us consider the main processes by which this can be done, neglecting now all possible depletions of the fundamental and the SH waves. The plane-wave equations that describe the effect of XPW generation, for which the terms that are responsible for possible losses by depletion and temporal and walk-off effects are neglected, have the following form:

$$\frac{dA}{dz} = 0, \tag{1a}$$

$$\frac{dS}{dz} = -i\sigma_1 A^2 \exp(i\Delta k_1 z), \tag{1b}$$

$$\frac{dB}{dz} = -i\sigma_2 SA^* \exp(-i\Delta k_2 z) - i\gamma AAA^* \exp(-i\Delta k_3 z), \tag{1c}$$

where S denotes the complex amplitude of the SH wave and A and B are the complex amplitudes of the two waves at the fundamental frequency with mutually perpendicular polarization vectors. Wave A is the input wave, and wave B is the generated XPW. $\sigma_1 = 2\pi d_{\text{eff,I step}}/(\lambda_1 n_2)$, $\sigma_2 = 2\pi d_{\text{eff,II step}}/(\lambda_1 n_1)$, and $\gamma = 6\pi\chi^{(3)}_{\text{eff}}/(8\lambda_1 n_1)$. The expressions for effective nonlinearities $d_{\text{eff,I step}}$, $d_{\text{eff,II step}}$, and $\chi^{(3)}_{\text{eff}}$ depend on the class symmetry of the crystal[46] and on the type of process[47] used and on the method of phase matching, e.g., birefringence or quasi-phase matching, and can be found from application of the following definitions:

$$d_{\text{eff,I step}} = \left[\frac{2}{\pi m'}\right]\frac{\langle \mathbf{e}_2\chi^{(2)}:\mathbf{e}_{1A}\mathbf{e}_{1A}\rangle}{2},$$

$$d_{\text{eff,II step}} = \left[\frac{2}{\pi m''}\right]\frac{\langle \mathbf{e}_2\chi^{(2)}:\mathbf{e}_{1A}\mathbf{e}_{1B}\rangle}{2},$$

$$\chi^{(3)}_{\text{eff}} = \left[\frac{2}{\pi m}\right]\langle \mathbf{e}_{1B}\chi^{(3)}:\mathbf{e}_{1A}\mathbf{e}_{1A}\mathbf{e}_{1A}\rangle.$$

The notation in brackets above has to be applied when quasi-phase matching (QPM) is used, where m is the order of the QPM interaction.

The wave-vector mismatches are defined as $\Delta k_1 = k_2 - 2k_{1A}$, $\Delta k_2 = k_2 - k_{1A} - k_{1B}$, and $\Delta k_3 = k_{1A} - k_{1B}$, where k_j are the wave vectors of the waves involved. Note that only two of the wave-vector mismatches are independent, because $\Delta k_2 - \Delta k_1 = \Delta k_3$. The last term of Eq. (1c) takes into account the contribution of the direct process of XPW generation that depends on the inherent cubic susceptibility of the nonlinear medium.

The general solution of Eqs. (1) when $S(0) = 0$ and $B(0) = 0$ gives, for wave amplitude B at the output of the nonlinear medium with thickness L,

$$B = |A|^2 A\left\{\frac{\sigma_1\sigma_2}{\Delta k_1}\frac{[\exp(-i\Delta k_2 L) - 1]}{\Delta k_2} + \gamma_{\mathrm{tot}}\frac{[\exp(-i\Delta k_3 L) - 1]}{\Delta k_3}\right\}, \tag{2}$$

where $\gamma_{\mathrm{tot}} = \gamma - \sigma_1\sigma_2/\Delta k_1$. The value of amplitude B depends strongly on the values of phase mismatch parameters Δk_1, Δk_2, and Δk_3. There are four possible situations in which a noticeable XPW signal can be observed at the output of the crystal. They correspond to specific phase-matched conditions: (a) $\Delta k_1 \approx 0$, (b) $\Delta k_2 \approx 0$, (c) $\Delta k_3 \approx 0$, and (d) simultaneously $\Delta k_1 \approx 0$ and $\Delta k_2 \approx 0$.

For condition (a) the process of SHG, $AA \rightarrow S$, is phase matched ($\Delta k_1 \approx 0$). XPW generation is the result of cascading from a TDSOP with the first step phase matched. Taking the limit $\Delta k_1 \rightarrow 0$ in Eq. (2) and using the relation $\Delta k_3 = \Delta k_2 - \Delta k_1$, we obtain

$$B(\Delta k_1 \approx 0) = -i\frac{\sigma_1\sigma_2}{\Delta k_2}|A|^2 AL\frac{\sin(\Delta k_1 L/2)}{(\Delta k_1 L/2)} \times \exp(i\Delta k_1 L/2 - i\Delta k_2 L) \tag{3}$$

As we can see from Eq. (3), the process of XPW generation is governed by the effective cascade-type coupling coefficient $\gamma_{\mathrm{casc},1} = \sigma_1\sigma_2/\Delta k_2$ and indicates that the process is cubic with respect to the input field.

For condition (b) the process of DFM, $SA^* \rightarrow B$, is phase matched ($\Delta k_2 \approx 0$). XPW generation is the result of cascading from a TDSOP with the second step phase matched:

$$B(\Delta k_2 \approx 0) = -i\frac{\sigma_1\sigma_2}{\Delta k_1}|A|^2 AL\frac{\sin(\Delta k_2 L/2)}{(\Delta k_2 L/2)} \times \exp(-i\Delta k_2 L/2). \tag{4}$$

The ratio between the intensity of the generated XPW and the intensity of the non-phase-matched SH wave for exact phase matching for the second process, $\Delta k_2 = 0$, is $|B/S|^2 = |\sigma_2 AL|^2$. This result is significant only when $|\sigma_2 AL| \ll 1$; otherwise, the generated cross-polarized intensity would be bigger than the SH intensity, a demonstration that the depletion of the SH wave that is due to the presence of the XPW has to be included.

In expressions (3) and (4), only the contributions of the phase-matched processes are included. The direct [$\chi^{(3)}$ dependent] non-phase-matched cubic process $AAA^* \rightarrow B$ is neglected; we take into account that $|\gamma/\Delta k_3| \ll |\sigma_1\sigma_2/\Delta k_3|L$. The proof of this inequality is given in the description of condition (d) below.

For condition (c) the process $AAA^* \rightarrow B$ is phase matched ($\Delta k_3 \approx 0$):

$$B(\Delta k_3 \approx 0) = -i\gamma_{\mathrm{tot}}|A|^2 AL\frac{\sin(\Delta k_3 L/2)}{(\Delta k_3 L/2)} \times \exp(-i\Delta k_3 L/2). \tag{5}$$

This situation is possible only if $\Delta k_3 = k_{1A} - k_{1B} \rightarrow 0$. This condition can be fulfilled, for example, in uniaxial crystals, if the fundamental wave propagates along the optical axis. At this phase-matching condition, when the medium is noncentrosymmetric the effect of XPW generation is a result of interference between the second-order cascaded cubic term governed by $\sigma_1\sigma_2/\Delta k_1$ and the contribution of the direct third-order process governed by γ. The two terms are of the same order of magnitude: In some crystals the cascaded term is bigger (see, e.g., Ref. 20); in others, the direct term is bigger (see, e.g., Ref. 17), and measurement of the efficiency of XPW generation in this phase-matched condition will in some cases permit the expression of third-order susceptibility tensor components in terms of second-order susceptibility tensor components.[10,11,16,18] Centrosymmetric and noncentrosymmetric crystals with $\chi^{(3)}_{1111}$ not equal to $3\chi^{(3)}_{1122}$ and nonvanishing $\chi^{(3)}_{1112}$ and $\chi^{(3)}_{1222}$ tensor components are suitable for observation of the $AAA^* \rightarrow B$ process with this phase-matching condition.[43] The case $\Delta k_3 \rightarrow 0$ is fulfilled automatically in any direction in cubic crystals and in biaxial crystals along the axes. The other possibility is to use QPM[47] in noncentrosymmetric crystals, creating in the crystal a QPM grating with period Λ such that $\Delta k_3 = k_{1A} - k_{1B} + (2\pi/\Lambda) \rightarrow 0$.

For condition (d), both SHG and DFM are simultaneously close to an exact phase-matching condition. For this case of double phase matching we have

$$B(\Delta k_1 = 0, \Delta k_2 = 0) = -|A|^2 AL\left(\frac{\sigma_1\sigma_2}{2}L + i\gamma\right). \tag{6}$$

XPW generation is the result of cascading from two phase-matched second-order processes. The contribution of the inherent cubic nonlinearity can be neglected because the inequality $|\sigma_1\sigma_2 L/2\gamma| \gg 1$ is well fulfilled. Indeed, taking advantage of the data for $\chi^{(3)}$ in BBO that were published in Ref. 48, one can get $|\sigma_1\sigma_2 L/2\gamma| \approx 15$. In this approximation the efficiency of XPW generation will depend on the crystal's length as L^4.

We can see that, in all the cases considered here, independently of the phase-matching conditions the amplitude of the XPW follows a cubic law dependence with respect to the input fundamental amplitude. Nevertheless, this consideration, as will be shown in Section 3, is valid only up to power levels for which $|\sigma_1 AL| < 1$ and $|\sigma_2 AL| < 1$.

It is clear from a comparison of the previously published treatments[10,11,49] of cascade phase-matched THG in quadratic media and from the simplified analysis pre-

Table 1. Schemes for XPW Generation in a Quadratic Medium

Case Designation	Input Wave	Step I SHG	Step II DFM	Equivalent Cubic Interaction
O1[a]	o	$o_1o_1 \rightarrow e_2$	$e_2o_1 \rightarrow e_1$	$o_1o_1o_1 \rightarrow e_1$
O2	o	$o_1o_1 \rightarrow o_2$	$o_2o_1 \rightarrow e_1$	$o_1o_1o_1 \rightarrow e_1$
E1	e	$e_1e_1 \rightarrow o_2$	$o_2e_1 \rightarrow o_1$	$e_1e_1e_1 \rightarrow o_1$
E2	e	$e_1e_1 \rightarrow e_2$	$e_2e_1 \rightarrow o_1$	$e_1e_1e_1 \rightarrow o_1$

[a] Realized in our experiment.

Table 2. Point Groups of Uniaxial Quadratic Crystals in Which Single-Crystal XPW Generation Is Possible

Point Group	Optimal Azimuthal Angle for the Processes $o_1o_1 - e_2, e_2o_1 - e_1$; $e_1e_1 - o_2, o_2e_1 - o_1$; $e_1e_1 - e_2, e_2e_1 - o_1$[a]	Optimal Azimuthal Angle for the Process $o_1o_1 - o_2, o_2o_1 - e_1$
$\bar{4}m2$	22.5°, 67.5°	Not possible
$3m$	Depends on ratio d_{22}/d_{31}	Depends on ratio d_{22}/d_{31}
$\bar{4}$	Depends on ratio d_{36}/d_{31}	Not possible
3	Depends on ratios d_{11}/d_{31} and d_{22}/d_{31}	Depends on ratio d_{11}/d_{31} and d_{22}/d_{31}
32	15°, 45°, 75°	15°, 45°, 75°
$\bar{6}$	Depends on ratio d_{22}/d_{11}	Depends on ratio d_{22}/d_{11}
$\bar{6}m2$	15°, 45°, 75°	15°, 45°, 75°

[a] We obtain optimal azimuthal angle φ by maximizing the product $|d_{\text{eff,I step}} d_{\text{eff,II } oee}|$.

sented here that a similarity exists between the processes of cascaded single-crystal THG and that of a single-crystal XPW generation. The difference is that in the case of THG the second step is sum-frequency mixing instead of DFM. Cascaded THG in $\chi^{(2)}$ media can be observed under the same phase-matching conditions as discussed above: $\Delta k_{\text{SH}} = k_2 - 2k_1 \approx 0$, $\Delta k_{\text{SFM}} = k_3 - k_2 - k_1 \approx 0$, and $\Delta k_3 = k_3 - 3k_1 \approx 0$. We would point out, however, that in some publications[11,20] it is wrongly stated that cascaded phase-matched THG is not possible when $\Delta k_{\text{SH}} \approx 0$.

Several uniaxial and biaxial crystal point groups can be host materials for cascaded XPW generation. We have analyzed uniaxial crystals. Combinations of the two different second-order processes that will generate a XPW in quadratic uniaxial nonlinear crystals are listed in Table 1. For negative uniaxial crystals (which correspond to most of the known quadratic crystals used in nonlinear optics) that utilize birefringence phase matching, only cases O1 and E2 (Table 1) are possible; for case E2 only, step II (DFM) can be phase matched. Cases O2 and E1 could be observed with birefringent positive uniaxial nonlinear crystals. So XPW generation will be possible in crystals that support type I and type II quadratic processes simultaneously; the uniaxial noncentrosymmetric point groups that are suitable for this type of support are listed in Table 2. One should judge the optimal polar angle for simultaneous type I and type II effective nonlinear coefficients. Note however that, of 21 noncentrosymmetric classes, 18 exhibit natural optical activity that may mask the effect of XPW generation.

Both birefringent phase-matching techniques and QPM[47,50–55] can be used for all methods of XPW generation listed in Table 1.

3. EFFICIENCY OF XPW GENERATION

The simplified analysis presented in Section 2 gives the overall conditions for nonlinear optical generation of XPWs but is not accurate for calculation of conversion efficiency in an actual experiment because of the effects of depletion. In fact, if the first step (SHG) is phase matched, the depletion of the fundamental wave has to be taken into account. If the second step is phase matched, the magnitude of the generated XPW is of the same order as that of the non-phased-matched SH wave generated in the first step. Then the depletion of the SH wave has to be taken into account. General plane-wave equations are written as (see e.g., Refs. 22 and 32)

$$\frac{\partial A}{\partial z} = -i\sigma_1 S A^* \exp(-i\Delta k_1 z) - i\sigma_2 S B^* \exp(-i\Delta k_2 z), \tag{7a}$$

$$\frac{\partial S}{\partial z} = -i\sigma_1 A^2 \exp(i\Delta k_1 z) - i2\sigma_2 A B \exp(i\Delta k_2 z) \tag{7b}$$

$$\frac{\partial B}{\partial z} = -i\sigma_2 S A^* \exp(-i\Delta k_2 z). \tag{7c}$$

In principle, Eqs. (7) should include four different coupling coefficients σ_i. However, neglecting frequency dispersion for index of refraction n_i and $\chi^{(2)}$, which is quite reasonable for the transparency band of the crystal, we reduce the number of the independent coupling coefficients to two: σ_1 and σ_2. We have omitted the term involving direct cubic nonlinearity because, as we pointed out in Section 2, it is important only when $\Delta k_3 \rightarrow 0$, a case not considered here in detail.

A. XPW Generation with Double Phase Matching

The case when both processes are phase matched is the most interesting situation from the application point of view, because in this case we can obtain maximum conversion into a XPW. Theoretically this case was considered by one of the present authors in Ref. 32, where almost 60% conversion was predicted when $\sigma_2/\sigma_1 = 1$. We moreover expect that by optimizing the ratio σ_2/σ_1 we can achieve conversion efficiency close to 100%. It is realistic to plan experiments with both steps phase matched, as several methods were recently proposed (for a review see Ref. 51) for simultaneous phase matching of two quadratic processes. For example, the method suggested in Ref. 52 uses a single quasi-phase-matched grating. Indeed, to achieve double phase matching one can employ first-order QPM for one of the parametric processes and third-order QPM for the second parametric process. An example of a quasi-phase-matched grating designed to generate a XPW in a periodically poled LiNbO3 sample is given in Ref. 32. Other methods of double phase matching use nonperiodic quasi-phase-matched structures, such as phase reversal quasi-phase matched[53] and periodically chirped quasi-phase matched[54] gratings. The structure made from quasi-periodic optical superlattices[13,14,55] that follow Fibonacci-type sequences can be employed for achieving simultaneous phase matching of several processes and therefore can be used as media for multistep SOC. Double phase matching in a broad spectral range can be achieved by use of uniform quasi-phase-matched gratings in a noncollinear geometry.[51] A promising environment for multiple phase matching and multistep cascading is furnished by two-dimensional nonlinear photonic crystals.[56,57] This type of nonlinear medium has a uniform index of refraction but a periodic two-dimensional variation of the sign of the second-order nonlinearity. This type of structure can support simultaneous phase matching of two and even three second-order nonlinear optical processes.[58–60]

As we have performed experiments in which we used a single crystal with birefringence phase matching for one of the steps, the theoretical analysis that follows is devoted to such cases.

B. Phase Matching for Second-Harmonic Generation

When only the first step, $\omega + \omega = 2\omega$, is phase matched, the intensities of the fundamental and the SH waves are much bigger than the intensity of the XPW; the influence of wave B on the fundamental and SH waves can therefore be neglected, and the system of Eqs. (7a) and (7b) can be solved separately. In conditions of exact phase matching ($\Delta k_1 = 0$), the SH wave grows according to $S(z) = A_0 \tanh(\sigma_1 A_0 z)$, and the fundamental wave amplitude follows $A(z) = A_0/\cosh(\sigma_1 A_0 z)$. It is clear that, at high conversion into a SH wave (when $|\sigma_1 A_0| L > 0.5$), the fundamental wave will be strongly depleted, and this will reduce conversion into a XPW. This is confirmed by the analytical formula obtained for the XPW conversion efficiency. By substituting the expressions for $S(z)$ and $A(z)$ into Eq. (7c) and integrating by parts, we get

$$|B/A_0|^2 = \left[\frac{\sigma_2 A_0 \tanh(\sigma_1 A_0 L)\,\mathrm{sech}(\sigma_1 A_0 L)}{\Delta k_2}\right]^2. \quad (8)$$

We show in Fig. 2 the conversion of the fundamental wave into a XPW as a function of dimensionless input amplitude $\sigma_1 A_0 L$ according to Eq. (8). Maximum conversion into a XPW is obtained for input intensities that correspond to a normalized value for $\sigma_1 A_0 L = 1.47$. It is interesting to note [Eq. (8)] that the dependence of the XPW intensity on the intensity of the fundamental wave is cubic at low input intensities and that this dependency afterward reaches a saturation level followed by decreasing efficiency owing to strong depletion of the fundamental wave.

For the dependence on conversion of the fundamental into a XPW with a slight deviation of the first step from the exact phase matching condition, Eqs. (7) are solved numerically; results are shown in Fig. 3. It can again be seen that at very high intensities the conversion into a

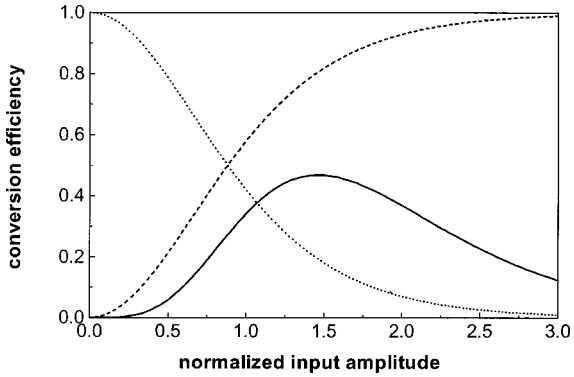

Fig. 2. Phase-matched first step. Conversion efficiency for the SH wave (dashed curve), XPW efficiency magnified $5(\Delta k_2 L)^2$ times (solid curve), and depletion of the fundamental intensity (dotted curve) as functions of dimensionless input amplitude parameter $\sigma_1 A_0 L$. Ratio $|\sigma_2/\sigma_1| = 0.53$.

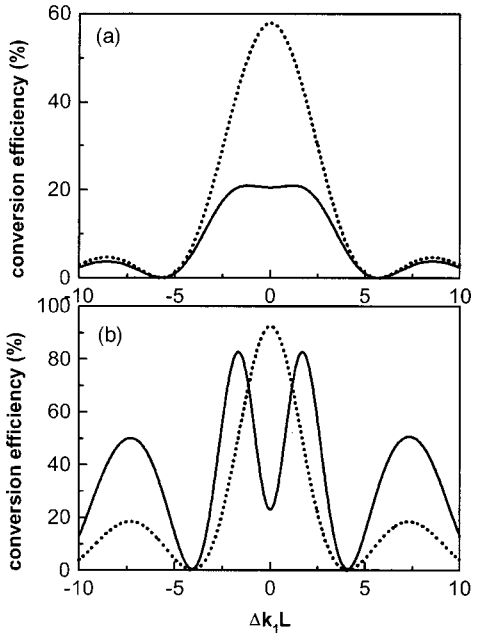

Fig. 3. Phase-matched first step. Conversion efficiency for the SH wave (dotted curves) and the XPW (solid curves) as functions of the detuning of the first step from exact phase matching for two values of the normalized input amplitude: (a) $\sigma_1 A_0 L = 1$, (b) $\sigma_1 A_0 L = 2$. The XPW efficiency is magnified $3(\Delta k_2 L)^2$ times. Ratio $|\sigma_2/\sigma_1| = 0.53$.

XPW tends to decline. At high input intensities the tuning curves have a deep peak in the center. The maximum for the XPW signal is not therefore located at the exact phase matching condition for the first step.

C. Phase Matching for Difference-Frequency Mixing

For phase matching for DFM ($\Delta k_2 \approx 0$) the generated SH wave is non-phase matched. Its amplitude is $\sim|\Delta k_1 L|^2$ times weaker than the fundamental amplitude (typically $|\Delta k_1 L| \sim 1000-10000$). The generated XPW has the same order of magnitude as the fundamental wave. The generated XPW and SH waves cannot have serious effects on the fundamental wave. For this reason it is acceptable to use the approximation of nondepletion of the fundamental wave, i.e., $\partial A/\partial z \approx 0$. Then Eqs. (7) can be solved exactly for arbitrary values of Δk_1 and Δk_2.

Indeed, Eq. (7) can be transformed into two separate second-order equations for waves $S(z)$ and $B(z)$:

$$\left(\frac{\partial^2}{\partial z^2} + i\Delta k_2 \frac{\partial}{\partial z} + 2\sigma_2^2 A^2\right) B(z) = -\sigma_1 \sigma_2 A^3 \exp(-i\Delta k_3 z), \quad (9)$$

$$\left(\frac{\partial^2}{\partial z^2} - i\Delta k_2 \frac{\partial}{\partial z} + 2\sigma_2^2 |A|^2\right) S(z) = -\sigma_1 \Delta k_3 A^2 \exp(i\Delta k_1 z). \quad (10)$$

Details of the derivation of Eqs. (9) and (10) are presented in Appendix A. Using $S(0) = 0$, $B(0) = 0$ and $A(0) = A_0$ as initial conditions, we find that the solutions of Eqs. (9) and (10) give, for conversion efficiencies $\eta_B = [B(L)/A_0]^2$ and $\eta_S = [S(L)/A_0]^2$, respectively,

$$\eta_B = \left(-\frac{\sigma_1 \sigma_2 A_0^2}{Q}\right)^2 \left\{\left[\frac{\delta k}{q}\sin\left(\frac{qL}{2}\right) - \sin\left(\frac{\delta k L}{2}\right)\right]^2 + \left[\cos\left(\frac{qL}{2}\right) - \cos\left(\frac{\delta k L}{2}\right)\right]^2\right\}, \quad (11)$$

$$\eta_S = \left(\frac{\sigma_1 A_0 \Delta k_3}{Q}\right)^2 \left\{\left[\frac{T}{q\Delta k_3}\sin\left(\frac{qL}{2}\right) + \sin\left(\frac{\delta k L}{2}\right)\right]^2 + \left[\cos\left(\frac{qL}{2}\right) - \cos\left(\frac{\delta k L}{2}\right)\right]^2\right\}, \quad (12)$$

where the following notation has been used: $Q = \Delta k_1 \Delta k_3 + 2\sigma_2^2 A_0^2$, $q = (\Delta k_2^2 + 8\sigma_2^2 A_0^2)^{1/2}$, $\delta k = 2\Delta k_1 - \Delta k_2$, and $T = \Delta k_2 \Delta k_3 + 4\sigma_2^2 A_0^2$.

Equations (11) and (12) can be simplified for exact phase matching for the second step ($\Delta k_2 = 0$) and when $|\Delta k_1| \gg |\sigma_2 A|$; this second condition was well fulfilled in our experiment ($\Delta k_1 = -8900\,\mathrm{cm}^{-1}$). Then, neglecting small-amplitude oscillating terms in Eqs. (11) and (12), we get

$$|B^2| \approx \frac{1}{2}\frac{\sigma_1^2 A^4}{\Delta k_1^2}\sin^2(\sqrt{2}\sigma_2 |A_0| L). \quad (13)$$

This type of formula was obtained previously [see Ref. 15, Eq. (3)] for cascading THG in a $\chi^{(2)}$ crystal, again demonstrating the similarity of the process of cascading XPW generation and cascading THG.

It is interesting to note that the ratio between the non-phase-matched SH intensity and the XPW intensity is constant. Indeed, besides exact phase matching for the second step, where $|\Delta k_2| > |\sigma_2 A_0|$, we can obtain

$$|S^2| \approx 4\frac{\sigma_1^2 A_0^4}{\Delta k_1^2}\sin^2\left(\frac{1}{2}\Delta k_1 L\right). \quad (14)$$

Comparing formulas (13) and (14), we can see that at the output of the crystal the ratio $|S/B|^2 = 8$ does not depend on pump intensity or on phase mismatch Δk_1 (this result is obtained when the two sine curves are taken at their maxima).

In Fig. 4 the theoretical angular dependencies for the XPW and the non-phase-matched SH intensities are shown for three levels of input power. The curves were plotted with the parameters of the experiment performed in a BBO crystal as described in subsection 3.D below. $\Delta k_2 = 0$ corresponds to phase-matching angle θ_{PM}. It has to be noted that the change of angle θ causes changes in both Δk_1 and Δk_2 phase-matching parameters. This is the reason for the fringe behavior of the non-phase-

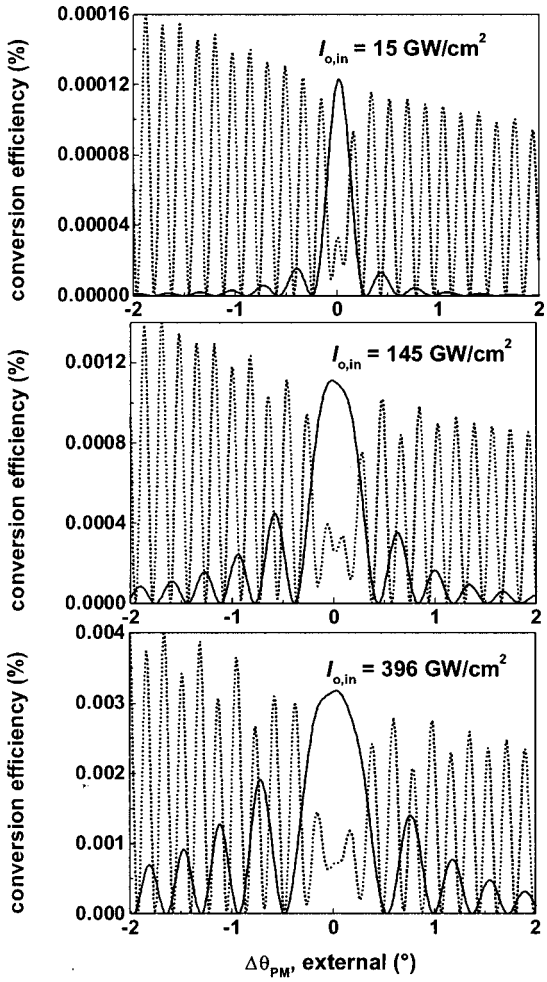

Fig. 4. Phase-matched second step. Theoretical predictions for XPW conversion efficiency, $\eta_B = I_B/I_A$ (darker curves) and SH signal, I_{SHG}/I_A (lighter curves) for deviation $\Delta\theta$ about the PM angle for type II SHG for three input intensities. Ratio $|\sigma_2/\sigma_1| = 0.53$; length of the BBO crystal, $L = 1.5$ mm. The curves for the conversion into SH wave S are divided by 8.

Table 3. Parameters of BBO Crystal Used for XPW Generation[a]

Point group	$3m$ negative uniaxial crystal
Transparency range	0.189–3.5 μm
Linear absorption coefficient at 532 nm	0.01 cm^{-1}
$d^{(2)}$ coefficients at 850 nm	$d_{22} = 2.3$ pm/V, $d_{31} = 0.04$ pm/V
$\chi^{(3)}$ coefficient at 850 nm	$\chi^{(3)} = 3.3 \times 10^{-22}\ m^2/V^2$
Type I SHG interaction	
Length of crystal	1 mm
Effective nonlinearity in phase-matching direction	$d_{\mathrm{eff},ooe} = d_{31}\sin\theta - d_{22}\sin(3\varphi)\cos\theta$
Phase matching and azimuthal angles	$\theta_{\mathrm{PM}} = 38.83°$, $\varphi = 15°$
Calculated refractive indices	$n_{o,620} = n_{e,310} = 1.6679273$
Calculated spectral width of the phase-matched curve (FWHM)	$\Delta\lambda_{\mathrm{PM}} = 1.5$ nm
Calculated internal angular width of the phase-matched curve (FWHM)	$\Delta\theta_{\mathrm{PM}} = 0.12°$
Walk-off angle	$\rho = 4.62°$
Aperture length	$L_a = d/\rho = 2.46$ mm
Group-velocity delay	$\nu_{1o-2e} = 378$ fs/mm
Nonstationary length	$L_{\nu,1o-2e} = \tau/\nu_{1o-2e} = 0.264$ mm
Type II SHG interaction	
Length of crystal	1.5 mm
Effective nonlinearity in phase matching direction	$d_{\mathrm{eff},eoe} = d_{\mathrm{eff},oee} = d_{22}\cos(3\varphi)\cos^2\theta$
Phase matching and azimuthal angles	$\theta_{\mathrm{PM}} = 58.33°$, $\varphi = 15°$
Calculated refractive indices	$n_{e,610} = 1.58006$, $n_{e,310} = 1.62399$
Calculated spectral width of the phase-matched curve (FWHM)	$\Delta\lambda_{\mathrm{PM}} = 1.1$ nm
Calculated internal angular width of the phase-matched curve (FWHM)	$\Delta\theta_{\mathrm{PM}} = 0.16°$
Walk-off angles	$\rho_{1o-1e} = 3.62°$, $\rho_{1o-2e} = 4.01°$
Aperture lengths	$L_{a,1o-1e} = 3.2$ mm, $L_{a,1o-2e} = 2.9$ mm
Group-velocity delays	$\nu_{1o-2e} = 172$ fs/mm, $\nu_{1e-2e} = 488$ fs/mm, $\nu_{1o-1e} = 316$ fs/mm
Nonstationary lengths	$L_{\nu,1o-2e} = 0.58$ mm, $L_{\nu,1e-2e} = 0.21$ mm, $L_{\nu,1o-1e} = 0.32$ mm

[a] Pump wavelength, 620 nm. Based on the data from Refs. 46, 48, and 61.

matched SH signal. One can see the depletion of the SH signal when a XPW is generated about phase-matching angle θ_{PM} for type II SHG. The theoretical phase-matched curves are slightly asymmetrical. One can also notice a broadening of the curves with increasing input amplitude.

D. Comparison of the Scheme with Phase-Matched Second-Harmonic Generation and the Scheme with Phase-Matched Difference-Frequency Mixing

For the scheme with the first step phase matched ($\Delta k_1 = 0$), the saturation intensity is defined by the condition $I \approx I_{\mathrm{cr},1}$, with $I_{\mathrm{cr},1} \approx 1.5(\varepsilon_0 cn/2\sigma_1^2 L^2)$. In contrast, the conversion efficiency into the XPW in the scheme with the second step phase matched ($\Delta k_2 = 0$) does not saturate; for input intensities $I < I_{\mathrm{cr},2}$ with $I_{\mathrm{cr},2} \approx \varepsilon_0 cn/4\sigma_1^2 L^2$ the XPW efficiency grows with quadratic law, and above this critical intensity the efficiency growth is linear. For the parameters of the BBO experiment described in Section 4 (see also Table 3), $I_{\mathrm{cr},1} = 8\ \mathrm{GW/cm^2}$ and $I_{\mathrm{cr},2} = 6.6\ \mathrm{GW/cm^2}$. The conversion efficiency is proportional to $(\Delta k_2 L)^{-2}$ when the first step is phase matched and to $(\Delta k_1 L)^{-2}$ when the second step is phase matched. That is why the choice of interactions with smaller mismatch for the non-phase-matched step is essential.

It is interesting to compare analytically the efficiency of the generation of XPW for various phase-matching conditions. We obtain the ratio $|B_2/B_1|^2$ of XPW intensity for $\Delta k_2 = 0$ versus XPW intensity for $\Delta k_1 = 0$ by combining formulas (8) and (13):

$$|B_2/B_1|^2 = \frac{1}{2}\left[\frac{\Delta k_2}{\Delta k_1}\frac{\sigma_1}{\sigma_2}\frac{\cosh(\sigma_1 A_0 L)}{\tanh(\sigma_1 A_0 L)}\right]^2. \qquad (15)$$

At high values of $|\sigma_1 A_0|L$ and comparable values for Δk_1 and Δk_2, XPW generation with the second step phase matched [condition (b)] is much more efficient. Indeed, in this limit ($|\sigma_1 A_0|L \gg 1$) Eq. (15) becomes

$$|B_2/B_1|^2 = \left(\frac{\Delta k_2}{\Delta k_1}\frac{\sigma_1}{\sigma_2}\right)^2 \exp(2|\sigma_1 A_0|L).$$

4. EXPERIMENTAL RESULTS AND DISCUSSIONS

For practical realization of a specific phase-matching condition for a XPW generation, we first used a BBO crystal cut for type II SHG ($e_1 o_1 \rightarrow e_2$) phase matching at the fundamental beam wavelength, $\lambda_1 = 620$ nm. We recall that $e_1 o_1 \rightarrow e_2$ and $e_2 o_1 \rightarrow e_1$ geometries are bound by the same phase-matching constraints. Generation of a XPW is the result of the cascading case labeled O1 in

Table 1. Taking into account that in BBO crystal $d_{15} \ll d_{22}$,[61] we can write the effective nonlinearities for type I and type II SHG as

$$d_{\mathrm{eff},ooe} \approx -d_{22}\sin(3\varphi)\cos\theta, \tag{16}$$

$$d_{\mathrm{eff},oee} = d_{22}\cos(3\varphi)\cos^2\theta. \tag{17}$$

The value of azimuthal angle φ ($\varphi = 15°$) was chosen to maximize the product $d_{\mathrm{eff},ooe}d_{\mathrm{eff},oee}$ and therefore ensure simultaneous action of the two steps.

The experimental setup is shown in Fig. 5. The parameters of the BBO samples used in the experiments are listed in Table 3. The input beam at $\lambda_1 = 620$ nm was produced by a colliding-pulse mode-locked dye system. The laser pulses used had the following parameters: duration, ~100 fs; energy, as much as 5 mJ, repetition rate, 10 Hz. The laser beam was focused with a lens ($f = 1.5$ m) that produced in the plane of the crystal a spot with $r = 0.2$ mm. To avoid depolarization in the crystal we tuned the input polarization (*o* wave) perpendicularly to the plane formed by the fundamental wave vector and the optical axis of the BBO crystal. In this way, the extinction ratio of the system polarizer–BBO crystal–analyzer, measured at relatively low input power, reduces to $R_X(0) = I_{\mathrm{bg}}/I_{o,\mathrm{in}} = 6 \times 10^{-6}$, where I_{bg} corresponds to background intensity. At the output of the crystal we also detected a non-phase-matched SH signal that was decreasing with increasing angle θ. Although the SH signal was non-phase matched, Maker fringes were not observed. When angle θ (the angle between wave vector **k** and the crystal axis) is tuned to $\theta_{\mathrm{PM}} = 58.33°$—the exact phase-matching value for $e_2o_1 \rightarrow e_1$ and $e_1o_1 \rightarrow e_2$—no additional SH signal can be detected: This is an additional check that only one ordinary, polarized wave is entering the crystal. From these initial conditions, an increase of the input power led to a worsening of the extinction ratio $R_X(I_{o,\mathrm{in}}) = R_X(0) + R_{\mathrm{NL}}(I_{o,\mathrm{in}})$, an indication that a new signal, polarized perpendicularly to the input wave, is generated by a nonlinear optical process in the crystal. In Fig. 6 the increase of the extraordinary component of the signal ($I_{e,\mathrm{out}} - I_{\mathrm{bg}}$) at the output of the system polarizer–BBO crystal–analyzer is shown as a function of the input intensity.

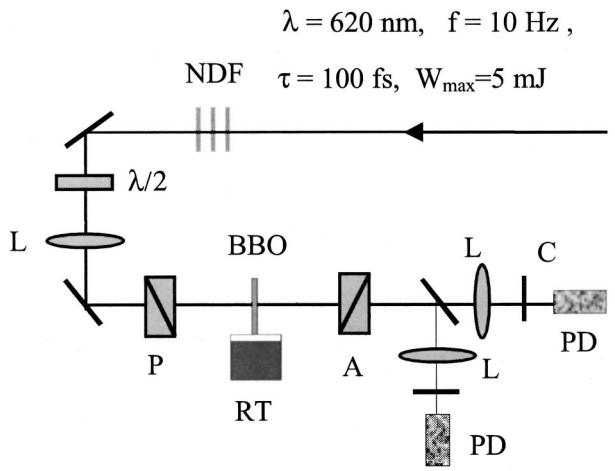

Fig. 5. Experimental arrangement: NDF, neutral-density filters; L's, lenses; P, polarizer; RT, three-axis rotational table; A, analyzer; C, color filter; PD's, photodiodes.

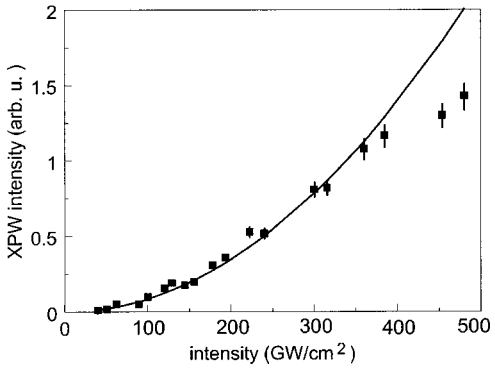

Fig. 6. Dependence of XPW signal ($I_{e,\mathrm{out}} - I_{\mathrm{bg}}$) on intensity of the input pump. Solid curve, quadratic fit to the experimental points that are recorded for $I_{o,\mathrm{in}} < 350$ GW/cm^2.

Special attempts have been made to define the power law of the generated XPW signal. The corresponding experimental curve is shown in Fig. 6. Formula (13) reveals that at low input intensity, when $|\sigma_2 A|L \ll 1$, the intensity of wave B has a cubic dependence on the fundamental wave intensity: $B \propto (\sigma_1\sigma_2/\Delta k_1)A^3L$. At higher input intensities, when $|\sigma_2 A|L > 1$, the dependence becomes quadratic. As a reference, for a BBO crystal, $|\sigma_2 A|L = 1$ corresponds to an input intensity of 13.2 GW/cm^2 when the relevant second-order component has a value $d_{22} = 2.3$ pm/V (Ref. 61) and the crystal length is 0.15 cm. Our experimental investigation of the dependence of XPW intensity on pump input intensity (Fig. 6) shows a quadratic dependence that is in good accordance with the prediction of formula (13). A similar experimental observation of a quadratic dependence for a cubic process is reported in Ref. 15, whose authors investigated THG in a single quadratic crystal.

The reason that we could not explore the range for which $|\sigma_2 A|L < 1$ is the presence of linear depolarization in the system polarizer–BBO crystal–analyzer. With specially chosen high-quality polarizers we expect a decrease in the magnitude of the extinction ratio; then the region of cubic dependence of this effect can be detected. The other possibility to explore the range $|\sigma_1 A_0|L < 1$ is to use crystals with higher nonlinearities.

The maximum efficiency of the generated XPW that is achievable for input intensities that are close to the damage threshold of the BBO crystal (500 GW/cm^2) was measured to be $R_{\mathrm{NL}} = 1.8 \times 10^{-5}$. At 500 GW/cm^2 and for $|\sigma_1 A|L = 12$ and $L = 0.15$ cm, formula (13) predicts a conversion efficiency into a perpendicular component equal to 4×10^{-5}, that is, twice bigger than the experimental measured efficiency. This agreement between experiment and theory can be considered a good one if one recalls that the theoretical analysis described in Section 3 has not taken into account either temporal and walk-off effects or possible losses.

We measured simultaneously both a XPW at fundamental frequency and SH signals when the crystal was tuned in a θ range from 56° to 60°. As expected, the magnitude of the XPW was sensitive to the deviation $\Delta\theta_{\mathrm{PM}} = \theta - \theta_{\mathrm{PM}}$ from the exact phase-matching angle. Results of these recordings are shown in Fig. 7. It can be clearly seen that the non-phase-matched SH signal that

results from $(o_1o_1 \rightarrow e_2)$ goes through a minimum at the angle of maximum XPW signal. This behavior, predicted by the theory, corresponds to depletion of the non-phase-matched SH wave that is due to the generation of the XPW. Moreover, as can be seen from the theoretical (Fig. 4) and the experimental (Fig. 7) curves, the general decrease of the non-phase-matched SH signal with increasing angle θ is related to the decrease in the coherence length for non-phase-matched type I SHG in the first step of this cascading interaction; in fact, an increase in θ for this process leads to an increase in the wave-vector mismatch. We have also plotted in Fig. 7 the SH intensity obtained with type II SHG measured separately when the two eigenpolarizations are present in the BBO crystal $(e_1o_1 \rightarrow e_2)$. The maximum of the XPW signal coincides with angle θ_{PM} at which type II SHG is expected to be maximal. This identical position is an additional support of our conclusion that the observed XPW signal results from cascading of two different second-order processes $(o_1o_1 \rightarrow e_2$ and $e_2o_1 \rightarrow e_1)$.

In contrast to the theoretical prediction (Fig. 4), the experimental dependence of the SH wave intensity on the deviation $\Delta\theta_{PM}$ (Fig. 7) does not contain Maker fringes. We remind the reader that in the system of differential equations used for the theoretical analysis presented in Section 3 the terms connected with the temporal and the spatial walk-off effects have been omitted; i.e., the theoretical analysis is valid for the cw plane-wave approximation when $L \ll l_{\mathrm{nst}}$ (l_{nst} is the figure of merit for the effects caused by temporal walk-off) and $L \ll l_a$ (l_a is the figure of merit for the effects caused by the spatial walk-off). In fact, as one can see from Table 3, the nonstationary lengths l_{nst} were smaller than the lengths of the crystals used, and obviously temporal walk-off effects cannot be neglected. At $L > l_{\mathrm{nst}}$ the group-velocity mismatch effect tends to wash out the fringe pattern.[62]

The influence of the input power and length of the BBO crystal on the width of phase-matched curve $\Delta\theta_{\mathrm{PM}}$ is illustrated in Fig. 8. A decrease in the BBO crystal's length at fixed input power leads to an increase of $\Delta\theta_{\mathrm{PM}}$. This behavior has its confirmation in our theoretical investigation. As can be seen from Fig. 8, a decrease in the input power results in a decrease of $\Delta\theta_{\mathrm{PM}}$, in accordance with the predictions from Eq. (11), as illustrated in Fig. 4.

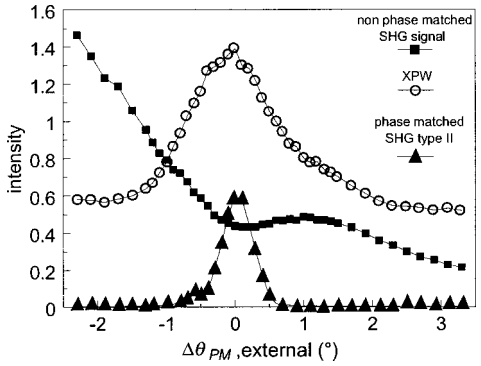

Fig. 7. Experimentally measured XPW signal and non-phase-matched SH signal as a function of the deviation $\Delta\theta$ from the phase-matched angle for type II SHG. Input power for these two curves, $I_{o,\mathrm{in}} \approx 300\ \mathrm{GW/cm^2}$. The lowest curve, taken with $I_{o,\mathrm{in}} \approx 30\ \mathrm{GW/cm^2}$, represents a phase-matched type II SHG signal measured in a separate experiment when the input polarizer was misaligned (both *o* and *e* waves enter the BBO crystal).

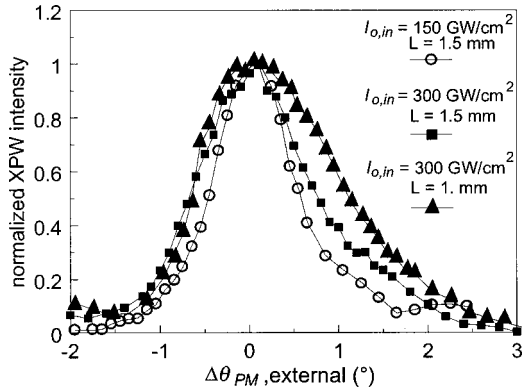

Fig. 8. Normalized XPW signal for three different sets of input power and crystal length.

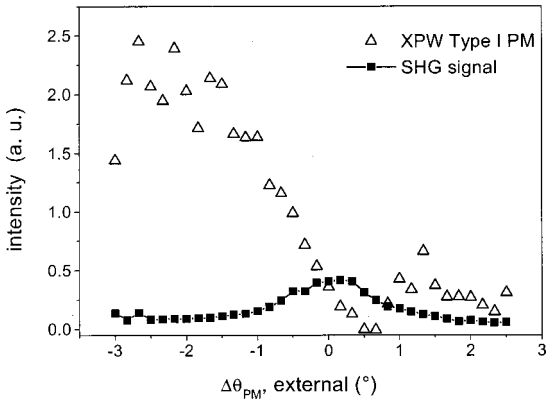

Fig. 9. Experimentally measured XPW signal and attenuated phase-matched SH signal as functions of deviation $\Delta\theta$ from the phase-matched angle for type I SHG. Input power, $I_{o,\mathrm{in}} \approx 350\ \mathrm{GW/cm^2}$.

As can be seen from relation (13), conversion efficiency of the fundamental wave into a XPW depends strongly on the magnitude of phase-mismatch parameter Δk_1. For the BBO experiment reported here, the magnitude of Δk_1 was dramatically high ($\Delta k_1 = 8900\ \mathrm{cm^{-1}}$), and this was the main reason for the low efficiency of conversion into a XPW. We have calculated that the same experiment performed in the infrared spectral region would yield a conversion efficiency 2 orders of magnitude higher. Of course, the best approach to achieving high conversion into a XPW is to use one of the methods for simultaneous phase matching for both second-order processes discussed in Subsection 3.A.

The experiment for measuring the effect of XPW generation with the first step phase matched was performed with a 1-mm-long BBO crystal cut for type I SHG, $\theta_{\mathrm{PM}} = 38.9°$, and azimuthal angle $\varphi = 15°$. The signal in this case was weaker than in the case of XPW generation in crystals cut for type II SHG. The angular dependence of the XPW signal is shown in Fig. 9. It can be seen to be qualitatively in agreement with the prediction shown in Fig. 3. We attribute the observed asymmetry to the interference between the generated XPW and the depolarized fundamental component at the input face of the crystal.

5. CONCLUSION

We have described theoretical and experimental investigations of phase-matched cross-polarized wave generation resulting from the simultaneous action of two different second-order processes in a single nonlinear medium. This four-wave mixing is fully degenerate in frequency but is nondegenerate with respect to the polarization state of the interacting waves. Like other cascading processes observed in quadratic media, the generation of a cross-polarized wave simulates a third-order process that is likely to be observed in centrosymmetric media.

We believe that the experimental and the theoretical work reported here will stimulate similar experiments with periodically poled media for which the efficiency would be much higher. In fact, effective nonlinearities in periodically poled $LiNbO_3$ and $LiTaO_3$ crystals are ~ 1 order of magnitude higher than the effective nonlinearity of the β-BaB_2O_4 crystal used in the present experiment.

If we do not restrict ourselves to single nonlinear medium, it is possible to generate efficient XPW in two nonlinear media, the first of them designed for phase-matched type I SHG and the second for phase-matched type II difference-frequency mixing. Each medium can be optimized separately for maximum efficiency (it is not necessary that the chosen media simultaneously support both processes, as it is in the case of a single-crystal device; therefore two different crystals can be used). The theoretical description is similar to the description of third-harmonic generation with two crystals. A double quasi-phase-matched grating structure upon a single substrate[63] is also a possible design for a double phase-matched device for efficient XPW generation.

All-optical switching and optical limiting could be some possible applications of the double phase-matched devices designed for efficient XPW generation.

APPENDIX A

For the derivation of Eqs. (9) and (10) we multiply Eq. (7b) by $\exp(-i\Delta k_2 z)$ and Eq. (7c) by $\exp(i\Delta k_2 z)$, and, differentiating the expressions obtained, we have

$$\left(\frac{\partial^2}{\partial z^2} - i\Delta k_2 \frac{\partial}{\partial z}\right) S + 2i\sigma_2 A \frac{\partial B}{\partial z} \exp(i\Delta k_2 z) = -\sigma_1 \Delta k_3 A^2 \exp(i\Delta k_1 z), \quad \text{(A1)}$$

$$\left(\frac{\partial^2}{\partial z^2} + i\Delta k_2 \frac{\partial}{\partial z}\right) B = -i\sigma_2 A \frac{\partial S}{\partial z} \exp(-i\Delta k_2 z). \quad \text{(A2)}$$

By replacing the derivatives $\partial B/\partial z$ and $\partial S/\partial z$ in Eqs. (A1) and (A2) with their equivalents, Eqs. (7c) and (7b), we obtain two separate second-order differential equations, Eqs. (9) and (10), for the SH amplitude and the XPW amplitude, respectively.

ACKNOWLEDGMENTS

The research described herein was performed within the Access to Research Infrastructure contract with the European Union (LIMANS III, CT-1999-00086). The authors are grateful to D. Shumov for growing several crystals. S. M. Saltiel thanks Yu. S. Kivshar for stimulating discussions. G. I. Petrov, N. Minkovsky, and S. M. Saltiel thank the Laboratoire d'Optique Appliquée for its kind hospitality and support during their stay and also the Bulgarian Science Fundation for partial support through grant 803.

S. M. Saltiel's e-mail address is saltiel@phys.uni-sofia.bg.

REFERENCES

1. G. Stegeman, D. Hagan, and L. Torner, "$\chi^{(2)}$ cascading phenomena and their applications to all-optical signal processing, mode locking, pulse compression, and solitons," Opt. Quantum Electron. **28**, 1691–1740 (1996).
2. G. Assanto, "Quadratic cascading: effects and applications," in *Beam Shaping and Control with Nonlinear Optics*, F. Kajzar and R. Reinisch, eds. (Plenum, New York, 1998), pp. 341–374.
3. S. Saltiel, I. Buchvarov, and K. Koynov, "Control of laser light parameters by $\chi^{(2)}$:$\chi^{(2)}$ cascading," in *Advanced Photonics with Second-Order Nonlinear Processes*, A. Boardman, L. Pavlov, and S. Tanev, eds. (Kluwer Academic, Dordrecht, The Netherlands, 1998), pp. 89–112.
4. R. DeSalvo, D. J. Hagan, M. Sheik-Bahae, G. Stegeman, E. W. Van Stryland, and H. Vanherzeele, "Self-focusing and self-defocusing by cascaded second-order effects in KTP," Opt. Lett. **17**, 28–31 (1992).
5. A. Dubietis, G. Valiulis, R. Danielius, and A. Piskarkas, "Fundamental-frequency pulse compression through cascaded second-order processes in a type II phase-matched second-harmonic generator," Opt. Lett. **21**, 1262–1264 (1996).
6. X. Liu, L. Qian, and F. Wise, "High-energy pulse compression by use of negative phase shifts produced by the cascade $\chi^{(2)}$:$\chi^{(2)}$ nonlinearity," Opt. Lett. **24**, 1777–1779 (1999).
7. A. V. Buryak and Yu. S. Kivshar, "Solitons due to second harmonic generation," Phys. Lett. A **197**, 407–412 (1995).
8. W. E. Torruellas, Z. Wang, D. J. Hagan, E. W. Van Stryland, G. I. Stegeman, L. Torner, and C. R. Menyuk, "Observation of two-dimensional spatial solitary waves in a quadratic medium," Phys. Rev. Lett. **74**, 5036–5039 (1995).
9. B. Bourliaguet, V. Couderc, A. Barthelemy, G. W. Ross, P. G. R. Smith, D. C. Hanna, and C. De Angelis, "Observation of quadratic spatial solitons in periodically poled lithium niobate," Opt. Lett. **24**, 1410–1412 (1999).
10. S. A. Akhmanov, L. B. Meisner, S. T. Parinov, S. M. Saltiel, and V. G. Tunkin, "Third order nonlinear optical susceptibilities of crystals; signs and amplitudes of the susceptibilities in crystals with and without inversion center," Zh. Eksp. Teor. Fiz. **73**, 1710–1728 (1977) [JETP **46**, 898–907 (1977)].
11. P. Qiu and A. Penzkofer, "Picosecond third harmonic light generation in β-BaB_2O_4," Appl. Phys. B **45**, 225–236 (1988).
12. I. V. Tomov, B. van Wonterghem, and P. M. Rentzepis, "Third harmonic generation in barium borate," Appl. Opt. **31**, 4172–4174 (1992).
13. S.-N. Zhu, Y.-Y. Zhu, and N.-B. Ming, "Quasi-phase matched third-harmonic generation in a quasi-periodic optical superlattice," Science **278**, 843–846 (1997).
14. Y.-Y. Zhu and N.-B. Ming, "Dielectric superlattices for nonlinear optical effects," Opt. Quantum Electron. **31**, 1093–1128 (1999).
15. X. Mu, X. Gu, M. V. Makarov, Y. J. Ding, J. Wang, J. Wei-,and Y. Liu, "Third-harmonic generation by cascading second-order nonlinear processes in a cerium-doped $KTiOPO_4$ crystal," Opt. Lett. **25**, 117–119 (2000).
16. P. S. Banks, M. D. Feit, and M. D. Perry, "High-intensity third-harmonic generation in beta barium borate through second-order and third-order susceptibilities," Opt. Lett. **24**, 4–6 (1999).

17. J. P. Fève, B. Boulanger, and Y. Guillien, "Efficient energy conversion for cubic third-harmonic generation that is phase matched in $KTiOPO_4$," Opt. Lett. **25**, 1373–1375 (2000).
18. Ch. Bosshard, U. Gubler, P. Kaatz, W. Mazerant, and U. Meier, "Non-phase-matched optical third-harmonic generation in noncentrosymmetric media: cascaded second-order contributions for the calibration of third-order nonlinearities," Phys. Rev. B **61**, 10,688–10,701 (2000).
19. V. V. Konotop and V. Kuzmiak, "Simultaneous second- and third-harmonic generation in one-dimensional photonic crystals," J. Opt. Soc. Am. **16**, 1370–1376 (2000).
20. Y. Takagi and S. Muraki, "Third-harmonic generation in a noncentrosymmetrical crystal: direct third-order or cascaded second-order process?" J. Lumin. **87–89**, 865–867 (2000).
21. K. Koynov and S. Saltiel, "Nonlinear phase shift via $\chi^{(2)}$ multistep cascading," Opt. Commun. **152**, 96–100 (1998).
22. S. Saltiel, K. Koynov, Y. Deyanova, and Yu. S. Kivshar, "Nonlinear phase shift resulting from two-color multistep cascading," J. Opt. Soc. Am. B **17**, 959–965 (2000).
23. Yu. S. Kivshar, A. A. Sukhorukov, and S. M. Saltiel, "Two-color multistep cascading and parametric soliton-induced waveguides," Phys. Rev. E **60**, R5056–R5059 (1999).
24. Yu. S. Kivshar, T. J. Alexander, and S. Saltiel, "Spatial optical solitons resulting from multistep cascading," Opt. Lett. **24**, 759–761 (1999).
25. I. Towers, R. Sammut, A. V. Buryak, and B. A. Malomed, "Soliton multistability as a result of double-resonance wave mixing in media," Opt. Lett. **24**, 1738–1740 (1999).
26. I. Towers, A. V. Buryak, R. A. Sammut, and B. A. Malomed, "Quadratic solitons resulting from double-resonance wave mixing," J. Opt. Soc. Am. B **17**, 2018–2025 (2000).
27. V. V. Konotop and V. Kuzmiak, "Double-resonant processes in $\chi^{(2)}$ nonlinear periodic media," J. Opt. Soc. Am. B **17**, 1874–1883 (2000).
28. G. Assanto, I. Torelli, and S. Trillo, "All-optical processing by means of vectorial interactions in second-order cascading: novel approaches," Opt. Lett. **19**, 1720–1722 (1994).
29. S. Trillo and G. Assanto, "Polarization spatial chaos in second harmonic generation," Opt. Lett. **19**, 1825–1827 (1994).
30. A. D. Boardman and K. Xie, "Vector spatial solitons influenced by magneto-optic effects in cascadable nonlinear media," Phys. Rev. E **55**, 1899–1909 (1997).
31. A. D. Boardman, P. Bontemps, and K. Xie, "Vector solitary optical beam control with mixed type I–type II second-harmonic generation," Opt. Quantum Electron. **30**, 891–905 (1998).
32. S. Saltiel and Y. Deyanova, "Polarization switching as a result of cascading of two simultaneously phase-matched processes," Opt. Lett. **24**, 1296–1298 (1999).
33. M. H. Chou, J. Hauden, M. A. Arbore, and M. M. Fejer, "1.5-mm-band wavelength conversion based on difference-frequency generation in LiNbO3 waveguides with integrated coupling structures," Opt. Lett. **23**, 1004–1006 (1998).
34. K. Gallo and G. Assanto, "Analysis of lithium niobate all-optical wavelength shifters for the third spectral window," J. Opt. Soc. Am. **16**, 741–753 (1999).
35. G. P. Banfi, P. K. Datta, V. Degiorgio, G. Donelli, and D. Fortusini, and J. N. Sherwood, "Frequency shifting through cascaded second-order processes in an *N*-(4-nitrophenyl)-L-prolinol crystal," Opt. Lett. **23**, 439–441 (1998).
36. G. I. Petrov, O. Albert, J. Etchepare, and S. M. Saltiel, "Cross-polarized wave generation by effective cubic nonlinear optical interaction," Opt. Lett. **26**, 355–357 (2001).
37. L. Lefort and A. Barthelemy, "Intensity-dependent polarization rotation associated with type II phase-matched second-harmonic generation: application to self-induced transparency," Opt. Lett. **20**, 1749–1751 (1995).
38. L. Lefort and A. Barthelemy, "All-optical transistor action by polarization rotation during type-II phase-matched second harmonic generation," Electron. Lett. **31**, 910–911 (1995).
39. I. Buchvarov, S. Saltiel, Ch. Iglev, and K. Koynov, "Intensity dependent change of the polarization state as a result of nonlinear phase shift in type II frequency doubling crystals," Opt. Commun. **141**, 173–179 (1997).
40. M. Asobe, I. Yokohama, H. Itoh, and T. Kaino, "All-optical switching by use of cascading of phase-matched sum-frequency generation and difference-frequency generation processes in periodically poled $LiNbO_3$," Opt. Lett. **22**, 274–276 (1997).
41. M. A. Krumburel, J. N. Sweetser, D. N. Fittinghoff, K. W. DeLong, and R. Trebino, "Ultrafast optical switching by use of fully phase matched cascaded second-order nonlinearities in a polarization-gate geometry," Opt. Lett. **22**, 245–247 (1997).
42. J. N. Sweetser, M. A. Krumburel, and R. Trebino, "Amplified ultrafast optical switching by cascading cascaded second-order nonlinearities in a polarization-gate geometry," Opt. Commun. **142**, 269–272 (1997).
43. N. I. Zheludev and A. D. Petrenko, "Physical mechanisms of nonlinear optical activity in crystals," Kristallografiya **29**, 1045–1052 (1985) [Sov. Phys. Crystallogr. **29**, 613–617 (1984)].
44. A. I. Kovrigin, D. V. Yakovlev, B. V. Zhdanov, and N. I. Zheludev, "Self-induced optical activity in crystals," Opt. Commun. **35**, 92–95 (1980).
45. M. G. Dubenskaya, R. S. Zadoyan, and N. I. Zheludev, "Nonlinear polarization spectroscopy in GaAs crystals: one- and two-photon resonances, excitonic effects, and the saturation of nonlinear susceptibilities," J. Opt. Soc. Am. B **2**, 1174–1178 (1985).
46. V. G. Dimitriev, G. G. Gurzadyan, and D. N. Nikogosyan, *Handbook of Nonlinear Optical Crystals* (Springer-Verlag, Berlin, 1999).
47. M. M. Fejer, G. A. Magel, D. H. Jundt, and R. L. Byer, "Quasi-phase matched second harmonic generation: tuning and tolerances," IEEE J. Quantum Electron. **28**, 2631–2654 (1992).
48. M. Sheik-Bahae and M. Ebrahimzadeh, "Measurement of nonlinear refraction in the second-order $\chi^{(2)}$ materials $KTiOPO_4$, $KNbO_4$, β-BaB_2O_4, and LiB_3O_5" Opt. Commun. **142**, 294–298 (1997).
49. G. I. Petrov, S. M. Saltiel, and A. B. Ivanova, "Measurement of $\chi^{(2)}$ components by comparing polarization resolved second-order cascade processes," in *ICONO'98: Nonlinear Optical Phenomena*, S. Chesnokov, V. Kandidov, and N. Koroteev, eds. Proc. Proc. SPIE **3733**, 112–120 (1999).
50. L. E. Myers, R. C. Eckardt, M. M. Fejer, R. L. Byer, W. R. Bosenberg, and J. W. Pierce, "Quasi-phase-matched optical parametric oscillators on bulk periodically poled $LiNbO_3$," J. Opt. Soc. Am. B **12**, 2102–2116 (1995).
51. S. M. Saltiel and Yu. S. Kivshar, "Phase-matching for nonlinear optical parametric processes with multistep-cascading," Bulg. J. Phys. **27**, 57–64 (2000).
52. O. Pfister, J. S. Wells, L. Hollberg, L. Zink, D. A. Van Baak, M. D. Levenson, and W. R. Bosenberg, "Continuous-wave frequency tripling and quadrupling by simultaneous three-wave mixing in periodically poled crystals: application to a two-step 1.19–10.71-μm frequency bridge," Opt. Lett. **22**, 1211–1213 (1997).
53. M. H. Chou, K. R. Parameswaran, M. M. Fejer, and I. Brener, "Multiple-channel wavelength conversion by use of engineered quasi-phase-matching structures in LiNbO3 waveguides," Opt. Lett. **24**, 1157–1159 (1999).
54. O. Bang, C. B. Clausen, P. L. Christiansen, and L. Torner, "Engineering competing nonlinearities," Opt. Lett. **24**, 1413–1415 (1999).
55. K. Fradkin-Kashi and A. Arie, "Multiple-wavelength quasi-phase-matched nonlinear interactions," IEEE J. Quantum Electron. **35**, 1649–1656 (1999).
56. V. Berger, "Nonlinear photonic crystals," Phys. Rev. Lett. **81**, 4136–4139 (1998).
57. N. G. R. Broderick, G. W. Ross, H. L. Offerhaus, D. J. Richardson, and D. C. Hanna, "Hexagonally poled lithium niobate: a two-dimensional nonlinear photonic crystal," Phys. Rev. Lett. **84**, 4345–4358 (2000).
58. S. Saltiel and Yu. S. Kivshar, "Phase matching in $\chi^{(2)}$ non-

linear photonics crystals," Opt. Lett. **25**, 1204–1206; erratum, 1612 (2000).
59. A. Chowdhury, S. C. Hagness, and L. McCaughan, "Simultaneous optical wavelength interchange with a two-dimensional second-order nonlinear photonic crystal," Opt. Lett. **25**, 832–834 (2000).
60. M. de Sterke, S. M. Saltiel, and Yu. S. Kivshar, "Efficient collinear fourth-harmonic generation by two-channel multistep cascading in a single two-dimensional nonlinear photonic crystal," Opt. Lett. **26**, 539–541 (2001).
61. I. Shoji, H. Nakamura, K. Ohdaira, T. Kondo, R. Ito, T. Okamoto, K. Tatsuki, and S. Kubota, "Absolute measurement of second-order nonlinear-optical coefficients of β-BaB_2O_4 for visible to ultraviolet second-harmonic wavelengths," J. Opt. Soc. Am. B **16**, 620–624 (1999).
62. S. A. Akhmanov and A. S. Chirkin, *Statistical Phenomena in Nonlinear Optics* (Moscow State U. Press, Moscow, 1971; in Russian).
63. Y. Deyanova, S. Saltiel, and K. Koynov, "Optimization of the process of frequency tripling and quadrupling in double grating quasi-phase matched structures," Opt. Commun. **178**, 437–447 (2000).